Sea bottom characteristics and geochemistry of oil and gas seeps in the Gulf of Mexico

John Decker[1], Philip Teas[2], Daniel Orange[3], and Bernie B. Bernard[4]

Abstract

From 2015 to 2018, TGS conducted a comprehensive multiclient oil and gas seep mapping survey in the Gulf of Mexico. The basis for identifying seeps on the sea bottom was a high-resolution Multi-Beam Echo Sounder survey, mapping approximately 880,000 km^2 of the sea bottom deeper than 750 m water depth, at a bathymetric resolution of 15 m, and a backscatter resolution of 5 m. We identified more than 5000 potential oil and/or gas seeps, and of those, we cored approximately 1500 for hydrocarbon geochemical analysis. The sea bottom features best related to hydrocarbon seepage in the GOM are high backscatter features, mud volcanoes, pock marks, brine pools, "popcorn" texture, fault traces, and anticlinal crests. We also tracked gas plumes in the water column back to the sea bottom to provide an additional criterion for hydrocarbon seepage. Cores from sea bottom targets recovered liquid oil, tar, and gas hydrates. Oil extract and gas analyses of samples from most target types produced values substantially higher than background in both oil and gas.

Introduction

The Gulf of Mexico (GOM) is an area well known to host natural hydrocarbon seepage (e.g., Bernard et al., 1976; Cole et al., 2001; De Beukelaer et al., 2003; MacDonald et al., 2015). From 2015 to 2018, TGS acquired high resolution bathymetry data from the entire GOM deeper than 750 m water depth. The survey was unique in that data collected and evaluated covered the entire deep water GOM allowing comparisons of different areas at a consistent high resolution. The survey was designed to identify possible natural hydrocarbon leakage on the sea bottom ("seep targets") and acquire piston cores from these targets for geochemical analyses. Seep targets were identified using Multi-Beam Echo Sounder (MBES) data and cored using, primarily, 6 m ultra short base line (USBL) navigated piston cores. Fugro acquired the MBES and subbottom profiler data; and TDI-Brooks acquired and analyzed the cores.

The sole purpose of this paper is to show the characteristics of representative seep targets on the sea bottom and the geochemical results from core samples from those features. The maps, images, and date shown in this paper are provided and approved by TGS. We are able to show in detail features of core targets and their geochemical results. We feel that this alone is a valuable contribution to the science of seep hunting. However, we were not allowed to show locations of seep targets or the regional distribution of the cores and their geochemical results, which are more related to commercial exploration in the GOM. The exploration significance of the images and data presented are left to the interpretation of the reader.

Background

The primary data used for seep detection acquired by MBES surveys include bathymetry, a measure of the water depth at any point, and backscatter, the strength of the returned sonar signal. In general, high backscatter results from the sonar signal encountering relatively hard or bathymetrically rough features on or just below the sea bottom. For example, sands and carbonates typically have higher backscatter than muds. Sea bottom mud typically acts as an acoustic sponge, dissipating the amplitude of the sonar signal, resulting in low backscatter. High backscatter features stand out as anomalies and are targets for further evaluation and sampling. One of the most important high backscatter anomalies, for seep hunting, is caused by chemosynthetic communities (Brooks et al., 1989). These communities form where hydrocarbon gas leaks to the sediment surface. The hydrogen sulfide associated with the seepage spawns a prolific bloom of sulfate reducing bacteria, which serve as the food source for mussels, tube worms, and other forms of animal life. Chemosynthetic

[1]ONE LLC, 500 Monte Cristo Pl. Cambria, CA 93428 USA. E-mail: john@seaseep.com (corresponding author).
[2]ONE LLC, 635 Gutshall Lane, Placerville, CO 81430 USA. E-mail: phil@seaseep.com.
[3]ONE LLC, 120 Rulofson St, Santa Cruz, CA 95060 USA. E-mail: dan@seaseep.com.
[4]TDI-Brooks International, Inc., TDI-Brooks International, Inc. (TDI-Brooks), USA. E-mail: berniebernard@tdi-bi.com.

Manuscript received by the Editor 3 March 2021; revised manuscript received 18 October 2021. ; published online 28 July 2020. This paper appears in *Interpretation*, Vol. 10, No. 1 (February 2022); p. 1–14, 24 FIGS.
http://dx.doi.org/10.1190/INT-2021-0065.1.

communities typically build topographic relief on the sea bottom that has a high backscatter signature due to the higher density and increased roughness caused by concentrations of carbonate shell fragments and diagenetic carbonate. Where these community complexes grow to be more than 50–100 m in diameter, we can generally see them with our MBES vessels typically traveling at 5–9 kt and surveying swaths 4–9 km wide. In addition to chemosynthetic communities, seep targets in the GOM include brine pools, tar flows, asphalt hard grounds, and mud volcanoes, which are discussed next. Water column anomaly (WCA) is sonar signal return emanating from within the water column. WCAs are caused by schools of fish, anchor chains, or certain other anomalous feature in the water column, but the main features of our interest are hydrocarbon gas plumes emanating from seeps on the sea bottom. By tracing the gas-related WCAs back to the sea bottom, we can usually find the source of the leaking gas and collect cores of the sediment near the origin of the plume. More than 3000 WCAs, interpreted to be gas plumes, were identified in the TGS GOM seep survey.

Methodology

The main purpose of MBES exploration surveys is to map the sea bottom and to identify possible seep targets for core sampling. In the TGS GOM seep survey, MBES sea bottom mapping was acquired by Fugro using Kongsberg EM302 and EM122 MBESs mounted on gondolas rigidly fixed to the hulls of the three different survey vessels. The higher frequency 30 kHz EM302 MBES system was used primarily in shallower water (approximately 500–3000 m water depth), and the 12 kHz EM122 was used primarily in deeper water (approximately 3000 to more than 4500 m water depth), although we did overlap the two systems in several areas for calibration and data comparison purposes. The 30 kHz signal attenuates faster in the water column than the 12 kHz, and as water depth increases, the higher frequency signal weakens to the point at which it is overcomed by ambient noise, primarily from the vessel. Different survey vessels, with different hull designs and ambient noise levels, lose meaningful sea bottom signal at different water depths. The cross-over water depth at which the signal to noise outweighs the higher frequency and greater resolving power of the 30 kHz ranges from approximately 2000 to 3000 m water depth.

In general, the GOM has an abundance of sea bottom features likely related to oil and gas seepage that were mapped on the MBES data. The final list of targets for core sampling was compiled from our own mapping, targets identified by the Fugro at sea team, and nominations from industry subscribers to the TGS program. Our goal in selecting targets for coring was to provide a broad regional distribution across a wide variety of target types. From our experience in other basins, which eventually also proved true in the GOM, similar core targets near one another generally result in similar geochemical results. By diversifying and broadening the core target distribution, we tend to expand the range of geochemical results and petroleum system interpretations. Figure 1 shows a multibeam backscatter map draped on bathymetry of the TGS seep survey area showing the locations of the piston core sites.

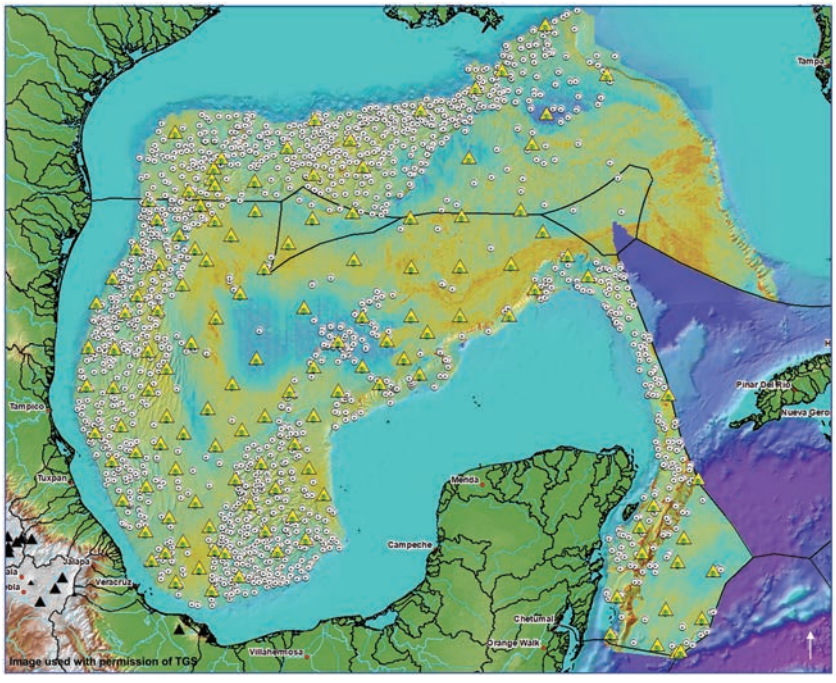

Figure 1. The MBES backscatter map of the GOM showing locations of piston cores. White dots are 6 m cores taken for screening geochemistry, acoustic calibration, and stratigraphic studies. The yellow triangles are 20 m JPCs taken off-target in areas not expected to be associated with hydrocarbon seepage to obtain background geochemical samples. Heat flow measurements also were taken at JPC locations.

The final inventory of potential seep targets was cored with 6.0 m long, 7.5 cm diameter core barrels. Off-target background samples were acquired on a grid along regional 2D seismic lines using 20 m long, 10 cm diameter Jumbo Piston Core (JPC) barrels. Conventional 6 m cores and JPCs were positioned at seep targets using USBL sonar navigation. With USBL navigation, the core barrel can be placed at the seabed laterally within 1% of the water depth and almost always within 25 m of the target. The average water depth for GOM cores was 1775 m and acquired cores averaged 11.6 m from the target or 0.76% of the water depth. With the 6 m core barrel, TDI-Brooks averaged 4.2 m of recovery. Harder substrates on the sea bottom, which is typical of our high backscatter

targets, generally had less recovery than coring muddy background substrate.

Cores acquired and returned to the coring vessel are cut into 1 m lengths. In general, three samples are taken for geochemistry from the bottom half of each core. If oil, tar, hydrates, etc. are observed through the clear core liner, additional samples are taken at those locations. Two types of samples were taken at each sample location within the core: (1) cans filled with one-third sediment, one-third sea water, and one-third air, for equilibrated head space (interstitial) gas analysis, and (2) bags of sediment for extraction and determination of the liquid hydrocarbon content. Both types of samples are frozen on board the vessel and remained in a frozen state until arriving at the TDI-Brooks laboratory for analysis.

For the GOM program, TDI-Brooks conducted thermogenicity screening measurements that included (1) the total scanning fluorescence (TSF) intensities from bagged sediment sections using dried-sediment extraction by solvent, (2) the C15+ hydrocarbons, by gas chromatography, in the same sediment extracts, and (3) the interstitial light hydrocarbon gas and CO_2 concentrations from the separately canned sediment sections (and sublimed gas hydrates) using wet-sediment gas partitioning and gas chromatography. From these analyses, screening the indicators of migrated liquid or gaseous thermogenic hydrocarbons were used to distinguish thermogenic seepage signals from background levels and diagenetic anomalies. To aid in this effort, stable carbon isotope ratios of consequential light hydrocarbon gas components of selected canned samples were determined. In addition, standard biological markers were determined on extracts of selected samples with TSF values exceeding analytical thresholds. Conclusions drawn from all results were used to compile a list of cores showing material and defensible evidence of at least traces of thermogenic oil and/or gas seepage. Conclusions also were drawn about age, maturity, and depositional environment of oil seepage from their biological marker determinations.

All of the cores from the Mexican GOM have been returned to the Mexican Government. All of the cores from the U.S. GOM have been archived at the TDI-Brooks facility in College Station, Texas. All geochemical and MBES data generated from the MBES and coring program in the GOM are proprietary commercial products of TGS. The data released in this report are with the permission of TGS.

Results: Coring and geochemistry

Overall, in the GOM program, 1479 cores were acquired, and 4443 geochemical samples analyzed for an average of 3.0 samples per core. Background cores were taken at 126 locations with the 20 m JPCs. The JPCs averaged 14.35 m of recovery. The primary purpose of the JPCs was to sample away from hydrocarbon targets to provide samples for background geochemical analyses. In addition, the JPCs were all logged, split, photographed, and sampled for biostratigraphy and evaluated for sedimentation rates. A grand total of 7775 m of core material was recovered.

The coring program was very successful in recovery of cores with indications of thermogenic hydrocarbon, including visible macroseepage.

- 200 cores recovered liquid oil
- 112 cores recovered heavy oil/tar/asphalt
- 333 cores showed evidence of gas expansion during depressurization
- 81 cores recovered gas hydrates
- 691 cores had an odor of H_2S (this indicates that the core had penetrated into the sulfate reduction zone, past the redox boundary, which allows for less biodegradation of any hydrocarbons sampled).

The geochemical results of the core sample analyses also were quite successful with most of the cores yielding geochemical indications of oil or thermogenic gas. Screening geochemical results are shown in Figures 2 and 3.

- 4443 samples were screened for C1–C5, CO_2, C15+, and TSF.
- 555 samples were analyzed for biological markers by GeoMark Research. Selection of these samples focused on those exhibiting at least traces of thermogenic liquid hydrocarbons during the screening process.
- 2942 gases were analyzed for stable carbon isotopes of selected components. Selection of these samples focused on those exhibiting thermogenic hydrocarbon gases during the screening process.

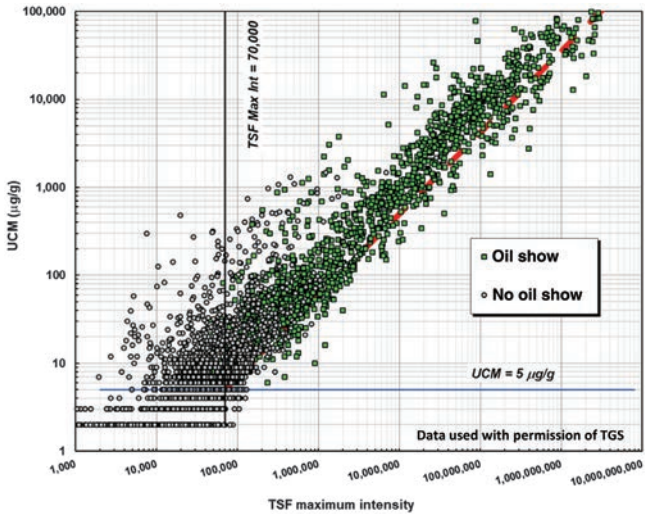

Figure 2. Extract plot (log-log) for all samples analyzed in the TGS GOM seep survey. The plot shows that samples containing seeping oil show a linear trend of increasing Unresolved Complex Mixture (UCM) with 9 increasing same-sample Total Scanning Fluorescence (TSF) Max Int (along the dashed yellow line).

- 2380 samples (53.6%) had TSF values more than 100,000 units, the empirically derived threshold value that we use for liquid hydrocarbon macroseepage and the likelihood of a sample yielding meaningful biological marker results.

The biomarker analyses and interpretations were provided by GeoMark Research in Houston, Texas. Biomarker results were correlated to known source rocks and production in the Greater GOM region. Source rock thermal maturity at generation, source age, and source facies also were interpreted from the biomarker results.

Numerous water column anomalies, which we interpreted as gas plumes, were identified in the MBES data from the GOM:

- 3276 gas plumes were interpreted from the MBES water column data.
- 191 plumes yielded repeat hits where the same plume was seen on two different MBES passes. The total unique seeps on the sea bottom generating gas plumes are therefore 3085.
- 268 of the plumes were cored, and 835 samples were analyzed for hydrocarbon geochemistry.

Seep target characteristics and geochemistry in the GOM

Sea bottom features associated with oil and gas expulsion (as well as gas plumes in the water column, and oil slicks on the sea surface, Garcia-Pineda et al., 2010) are all common in the GOM, but they are mostly concentrated in a C-Shaped arc from the northern to the western U.S. GOM, and into the western and southern Mexico GOM. They are closely associated with sea bottom features related to salt diapirism and neo-tectonics

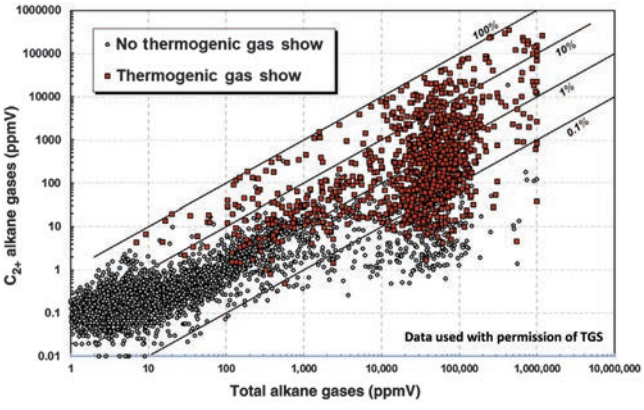

Figure 3. Gas wetness plot (log-log) for all samples analyzed in the TGS GOM seep survey. The plot illustrates the composition range of alkane light hydrocarbons in the sediments and hydrates of this study by comparing the values of the nonmethane (C_{2+}) fraction with the methane-included total gas for each analyzed core section. We have drawn diagonal lines showing where decade steps in percentages of C_{2+} in a sample would plot. Note that the analyses are reported by volume rather than by mass.

and largely missing from the central deepwater GOM, which is likely underlain by oceanic crust (Davison et al., 2021).

Based on the percentage of cores with indications of hydrocarbons and the percentage of samples with geochemical indications of hydrocarbons, relative to other basins evaluated with similar programs, much of the GOM can be considered a target-rich environment for seepage. The GOM also provides a wide variety of target types, some not seen in other basins, and the gamut of hydrocarbon types from biogenic or thermogenic gas, to live oil and tar fields. The sea bottom features determined to be most successfully sampled and shown to be related to hydrocarbon seepage in the GOM are

- high backscatter circular features with or without bathymetric expression
- high backscatter features with flow appearance
- mud volcanoes
- pock marks
- brine pools
- popcorn texture
- fault traces
- anticlinal crests.

Water column gas plumes also pointed to one of the above sea bottom features and supported our precore interpretations that the feature was likely related to hydrocarbon seepage.

Note that all color MBES maps in this section are of quantitative multibeam backscatter using the same high-low color palette range. Backscatter data display the strength of the returned sonar signal in dB. The blue color represents approximately two standard deviations below the mean dB level in the GOM, and the red represents approximately two standard deviations above the mean. Quantitative means that the dB range is fixed for the entire program, so red, for example, is the same dB level on all figures.

High backscatter circular features

Circular or semicircular high backscatter features on the sea bottom may occur with or without topographic relief. The circular character is generally caused by a point source of seepage at the sea bottom. Figure 4 shows a circular feature of high backscatter, approximately 300 m in diameter with a height of approximately 50 m above the local sea bottom surrounded by a shallow moat of <5 m depth. This feature displays obvious contrast with the generally low speckled backscatter of normal marine mud. The piston core from this feature was oil stained and contained tar. The geochemistry contained wet gas with only 30.3% methane and extremely high (hundreds of millions) TSF values.

Figure 5 shows a relatively subtle area of high backscatter, approximately 150 m in diameter with a more nebulous boundary and irregular shape. An initial core yielded significant hydrocarbon, and we took the oppor-

tunity to return to the area to acquire three additional cores — one in the same feature, but closer to the edge, and two at progressively farther distance from the anomalous backscatter. Of the two cores taken in the high backscatter, one contained tar fragments, both had TSF values greater than 100 million, and both contained wet gas ranging from 50% to 75% methane. Cores taken 50–100 m from the high backscatter target had substantially lower TSF values and no anomalous gas.

High backscatter flow features

Another common feature in basins with robust seepage, like the GOM, is high backscatter with a flow-like appearance. Similar to circular features, we interpret flow features to be hydrocarbon seepage emanating from a point source. Where the point source of the seep occurs on sloping sea bottom, the seep fluids appear to flow down slope to deeper bathymetric levels. We generally interpret the high backscatter to be the result of chemosynthetic communities affecting the acoustic properties of the sea bottom and/or an increase in hardness or roughness of the flow material relative to the surrounding seafloor (note that in some basins, the high backscatter flow pattern occurs on the flanks of mud volcanoes and the cores from the flows contained rock fragments, which contribute to the high backscatter acoustic signal; these were not observed in the GOM). In general, flow textures show little or no bathymetric expression; that is, the flow itself is not elevated measurably above the background slope.

Figure 6 shows a good example of an approximately 3 km long high backscatter flow pattern with virtually no bathymetric expression. Our interpretation is that the flow was initiated from a point source high on the flank of the channel margin, progressed downslope to the northwest to the channel floor, turned westward and continued down channel. Although the backscatter contrast with the surrounding sea bottom is strong, the geochemical results from this location were only modest. Core geochemistry showed low amounts (total

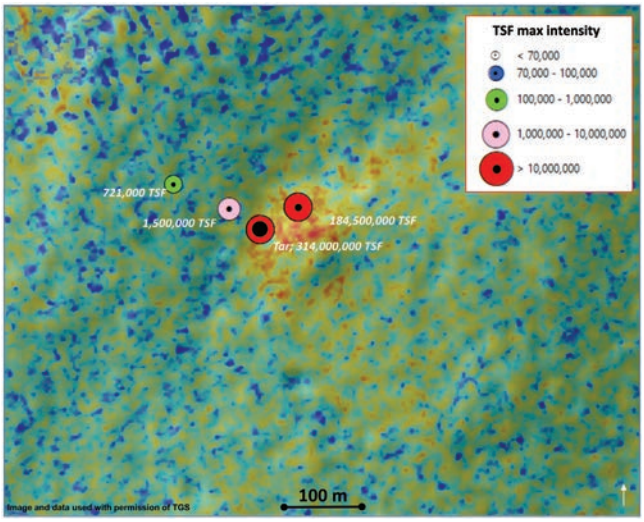

Figure 5. The MBES backscatter map showing moderately high to high backscatter with vague boundaries. The first core taken near a SAR slick, and recovered oil-stained clay with a strong H_2S odor. The core had extremely high TSF values. Later in the program the site was revisited to evaluate the geochemical characteristics progressively farther from the backscatter anomaly. An additional confirmation core was taken in the high backscatter zone and then two more cores taken 50 and 73 m from the first.

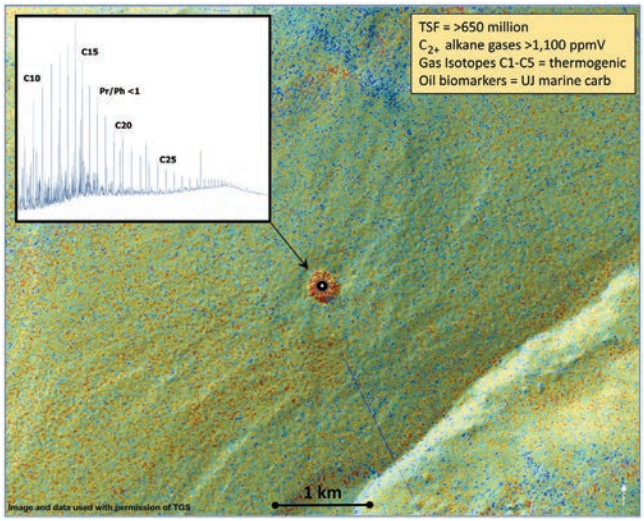

Figure 4. The MBES backscatter map of almost perfectly circular mound 300 m in diameter with a very distinct high backscatter anomaly. Core from this location recovered >1.2 m of very soupy silty clay with liquid oil and abundant tar fragments.

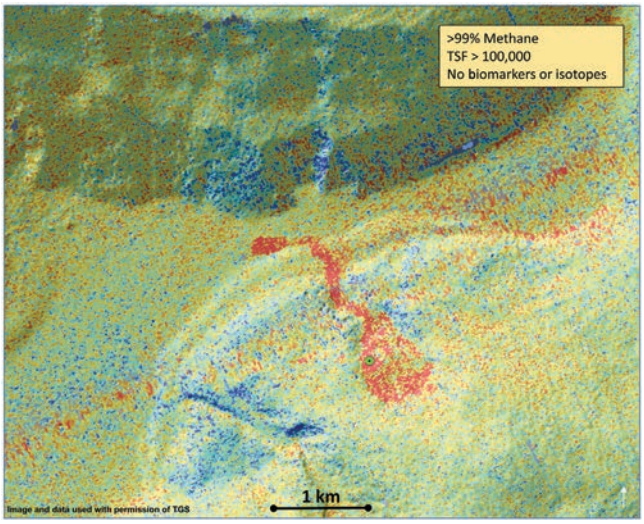

Figure 6. The MBES backscatter map of high backscatter area with flow pattern extending from up slope to the south-southeast to down slope to the north-northwest. One core was taken near the presumed source of the flow. The core recovered predominantly soft olive brown to green gray clay with common black organic fragments.

alkane gases up to approximately 180 ppmV) of dry gas with more than 99% methane and a TSF value of just more than 100,000.

Similarly, Figure 7 shows another high backscatter flow pattern. Our interpretation is that the flow was initiated from a point source to the south and flowed northward downslope. Three cores were taken from this feature, one near our presumed source and two near the presumed terminus. All cores show moderate gas values with total alkane gases of >800,000 ppmV and methane ranging from 94% to 98%. TSF oil extracts values ranged from fairly low (<100,000) to just more than 1 million. Curiously, the highest TSF value was obtained from just outside the high backscatter flow.

Mud volcanoes

Mud volcanoes are generally circular to semicircular, positive relief features on the sea bottom, formed by eruption of fluidized sediment, and can occur with or without high backscatter. Mud volcanoes may typically exhibit any or all of the following features: concentric rings around a central vent, a caldera or collapsed center, a moat or circular depression around the positive relief feature, and radial flow patterns trending from the central vent down slope. In many ways mud volcanoes resemble igneous volcanoes, hence the name, but generally with gentler slopes. Mud volcanoes form due to locally high fluid pressures causing a mud diapir that brings a slurry of mud, sand, and rock fragments to the sea bottom, creating a positive relief feature resembling an igneous volcano (Newton et al., 1980).

Mud volcanoes are not particularly common in the GOM with less than 30 having been cored in this program, but they do exist where high sediment loads produce overpressure and/or where oil and gas fluid pressures exceed lithostatic pressures. Mud volcanoes are most always good candidates for hydrocarbon macroseepage.

Figure 8 shows a roughly circular mud volcano with what we interpret to show two episodes of growth, an initial phase with a caldera collapse and a second phase of growth within the caldera. We acquired one core in the central high backscatter interpreted to be a vent area, which yielded oil and thermogenic gas. Total alkane gases ranged from 20,000 to 29,000 ppmV and consisted predominantly of methane (>98.6%). The C_1–C_5 (methane through n-pentane alkanes) carbon isotopes ranged from −19.8‰ (pentane) to −35.1‰ (methane) and were all qualified as thermogenic by TDI-Brooks. TSF values were very high, with all samples in the 400,000 range. GeoMark Research biomarker analysis suggests that the source of the oil is from a Tertiary paralic/deltaic shale source rock.

Figure 9 shows another example of a well-defined circular mud volcano with a slight moat and a more irregular surface relief and high backscatter. Two water column anomalies in the MBES data were projected to be emanating from the feature. Core geochemistry had high TSF values in all three samples (all in the tens of millions). Alkane gases totaled 50,000 and 85,000 ppmV and were all >99% methane. The tar was biodegraded, and GeoMark was unable to type the source facies.

Pock marks

Pock marks are generally concave circular features with negative bathymetric relief, i.e., pits on the sea bottom (MacDonald et al., 1990; Scanlon et al., 2005). They can occur individually or, more typically from our

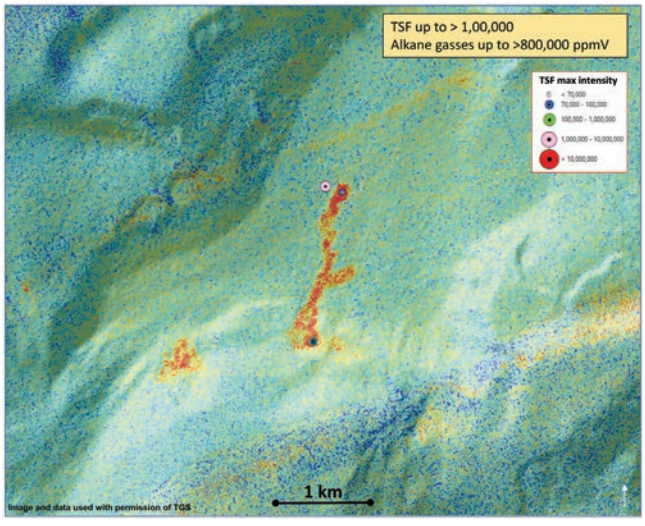

Figure 7. The MBES backscatter map showing very distinct high backscatter area with flow pattern extending from up slope to the south-southwest to down slope to the north-northeast. One core was taken near the presumed source of the flow to the south, and two additional cores were taken near the apparent terminuses of the flow to the north. All cores recovered mainly green gray clay to silty clay.

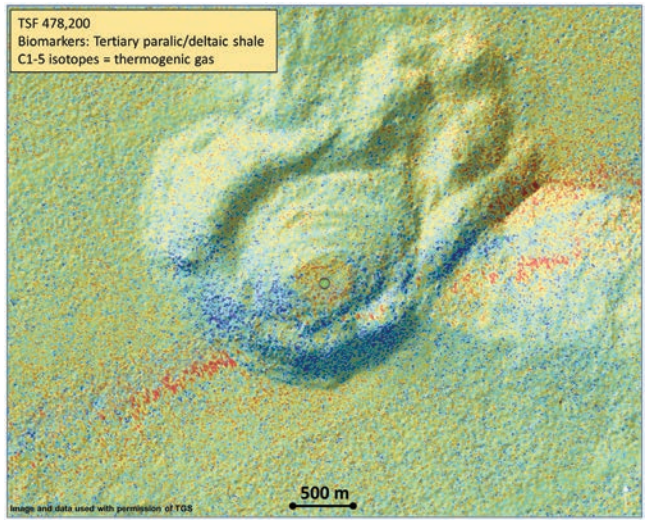

Figure 8. The MBES backscatter map showing well-defined mud volcano 2.5 km in diameter with moderate backscatter on a relatively flat crest approximately 400 m in diameter. The core recovered green gray clay with moderate H_2S odor and gas expansion fractures.

experience, in fields or trends of up to dozens of pits. Pock marks may exhibit high backscatter, generally near the center, but more typically exhibit little or no anomalous backscatter. Pock marks in the GOM are generally less than 250 m in diameter and are less than 10 m deep. Rarely, large circular depressions can exceed 1 km in diameter and can be over 100 m deep. Globally, from our experience, pock mark core geochemistry tends to be higher in gas than oil. In the GOM, however, pock marks may yield significant oil geochemistry, and cores from pock mark features locally encountered tar. Of the 258 samples from pock marks collected with GOM cores, TSF averaged more than 50 million. Excluding the 21 samples with tar, the TSF still averaged more than 15 million. The average total alkane gases from pock mark samples were more than 15,000 ppmV of wet gas, with methane accounting for only 81.6% of the total gas composition.

Figure 10 shows two typical pock marks from the GOM. They both have small high backscatter areas near the center of the pock mark. The one on the left was cored and recovered tar with TSF > 500 million and background levels of hydrocarbon gas. GeoMark Research biomarker data allowed the tar from this location to be correlated to produced oil from Upper Jurassic marine carbonate source rocks.

Figure 11 shows a pock mark field with about a dozen pock marks averaging approximately 150 m in diameter. We targeted a relatively small patch of anomalously high backscatter on the flank of one pock mark. The three core samples had relatively high total alkane gases ranging from 15,000 to more than 53,000 ppmV, consisting predominantly of methane (>98.8%). C_1–C_5 carbon isotopes ranged from −17.4‰ (pentane) to −55.0‰ (methane) and were qualified by TDI-Brooks to be of thermogenic origin. TSF values were extremely high, ranging from 2.7 to more than 219 million. The highest TSF sample was analyzed for biomarkers but proved too severely biodegraded to provide any meaningful source facies interpretations. Perhaps interestingly, the CO_2 from the three core samples ranged from 35,000

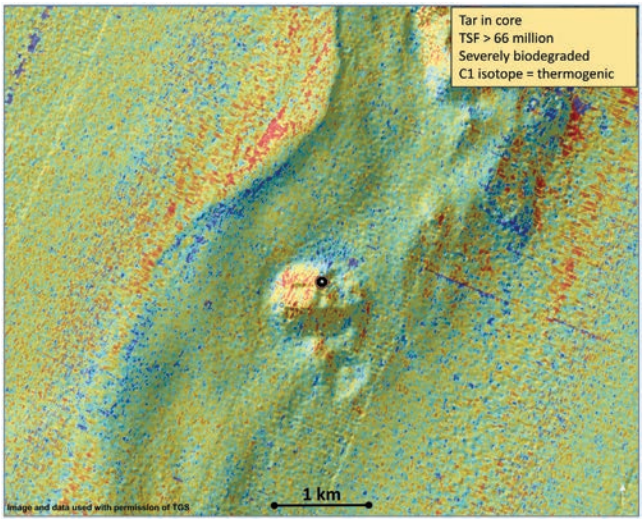

Figure 9. The MBES backscatter map showing well-defined mud volcano approximately 1 km in diameter with moderately high backscatter. One core placed at the black dot near the crest consisted of gray sandy mud with rock fragments, including tar, with moderate H_2S odor, and live oil staining.

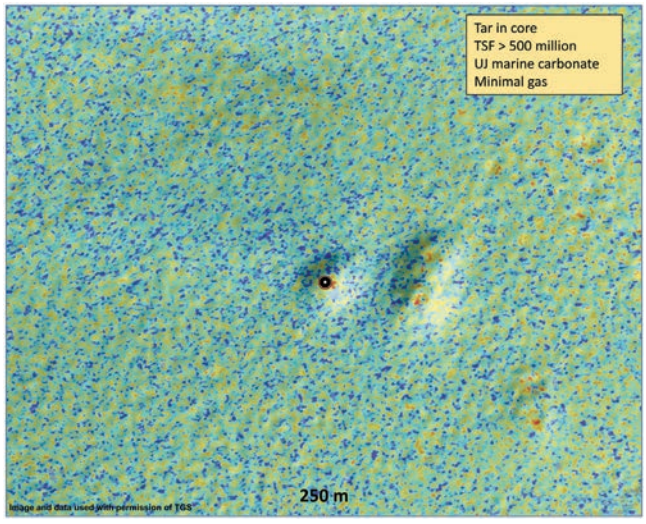

Figure 10. The MBES backscatter map showing two well-defined pock marks, each approximately 250 m in diameter. Both pocks have slightly elevated mini-domes with moderately high backscatter in their centers. One core taken in high backscatter center of the Western pock recovered gray mud with chunks of tar and a distinct petroleum smell.

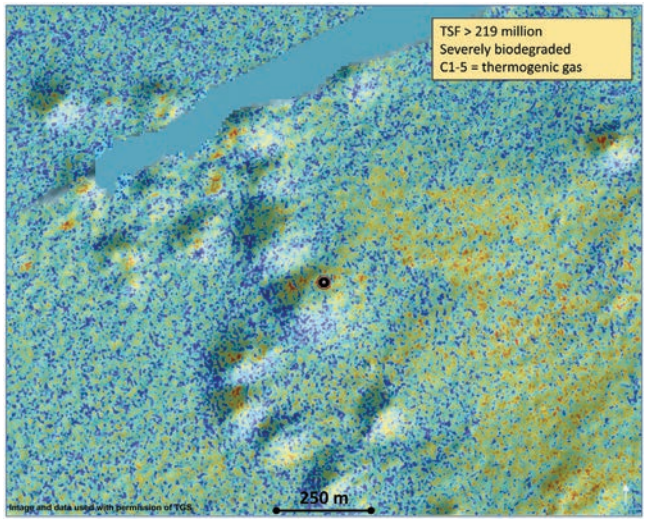

Figure 11. The MBES map showing pock mark field with overall generally low backscatter. One core was taken in relatively high backscatter area on the flanks of one of the larger pocks. The core consisted of green gray clay, which had a strong H_2S odor. Although liquid oil was not recognized in the field while processing the core, later in the heat of a Texas summer, tar with the viscosity of tooth paste was observed escaping from one of the core sections.

to more than 60,000 ppmV, much higher than the GOM average from the TGS program of 7775 ppmV.

Figure 12 shows the largest circular depression observed in the GOM in the TGS survey. The feature is 1.8 km in diameter and 248 m deep. Total alkane gases range from under 10 to more than 400 ppmV, but they were generally in the background levels. The two samples with the highest total alkane values were >99.7% methane and classified as biogenic by TDI-Brooks. Extract geochemistry yields TSF values more than 1 million. GeoMark Research biomarker data suggest that the source of the extracted oil is Tertiary paralic/deltaic shale. We offer no interpretation for the origin of this one-of-a-kind depression in the GOM.

Brine pools

Brine pools are deepwater lakes on the sea bottom with high concentrations of salt that is of significantly higher density than normal sea water (MacDonald et al., 1990). Brine pools in the GOM (Brooks et al., 1979; Joye et al., 2005) are typically associated with exposed or near sea-bottom salt, hydrocarbon gas, and chemosynthetic communities. Our data show that the brine pools also are associated with high oil geochemical indicators, with tar commonly recovered in the core barrel.

Figure 13 shows an interpreted brine pool with a very low backscatter center (brine lake) and high backscatter rim. The contour interval is 10 m, and the contour lines show that what we interpret as the rim of the brine lake is at about the same depth around the perimeter of the low backscatter feature. Cores from the low backscatter center and high backscatter rim recovered tar. Core sample geochemistry produced exceptionally high TSF values, which are to be expected when analyzing tar, and modest to low total alkane gases ranging from approximately 100 to 600 ppmV wet gas with low methane values, ranging from approximately 50% to 80% of total alkane gases. Gas carbon isotopes ranged from −28.4‰ (pentane) to −39.4‰ (ethane), and methane was −32.9‰. Cores were not analyzed for inorganic compounds.

Figure 14 shows another example of an interpreted brine pool with a low backscatter center and high backscatter rim. The transition from very low to very high backscatter occurs at about the same depth around the perimeter of the low backscatter feature. This is consistent with our interpretation that this feature is a brine pool. As with the brine pool features shown in Figure 13, the low backscatter center and high backscatter rim recovered tar. TSF values were in the billions with modest amounts of gas. Total alkane gases were approximately 2500 ppmV with both biogenic gas, having methane content of >99.9%, and thermogenic gas, based on C_1–C_5 isotope data. The figure also shows what we interpret as paleo brine lakes outlined by their high backscatter rims. Note the curious field of small mounds south of the core locations. This is an example of a feature that will be defined and discussed in the next section.

Popcorn texture

Popcorn texture is an informal name given to a feature observed in several areas of the GOM, but which

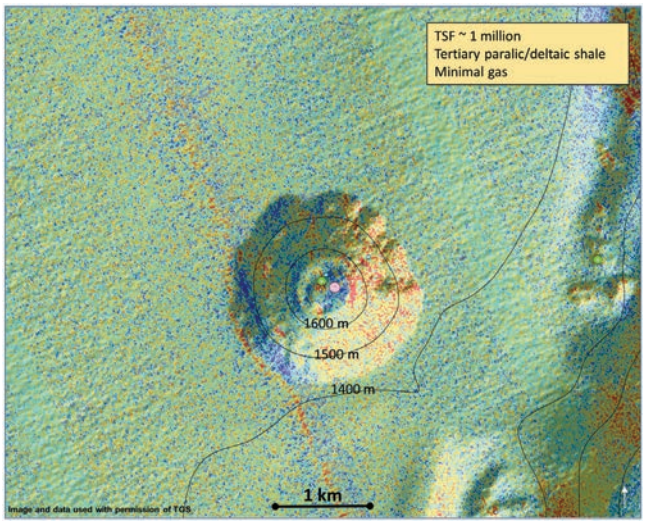

Figure 12. The MBES backscatter map of a "Super Pock" 1.8 km in diameter and 248 m deep. Because of the orientation of the slopes of the pock relative to the ship track, the high backscatter facing the boat and the low backscatter facing away from the boat are questionable at best and were disregarded in our core target selection. The tiny semicircular high back scatter patches on the bottom of the depression were, however, of particular interest because one coincided with a projected touchdown point of a gas plume in the water column. Two cores were taken at the base of the depression, one in high backscatter and the other in very low backscatter, for comparison purposes. Both cores consisted of dark green gray mud with similar geochemistry.

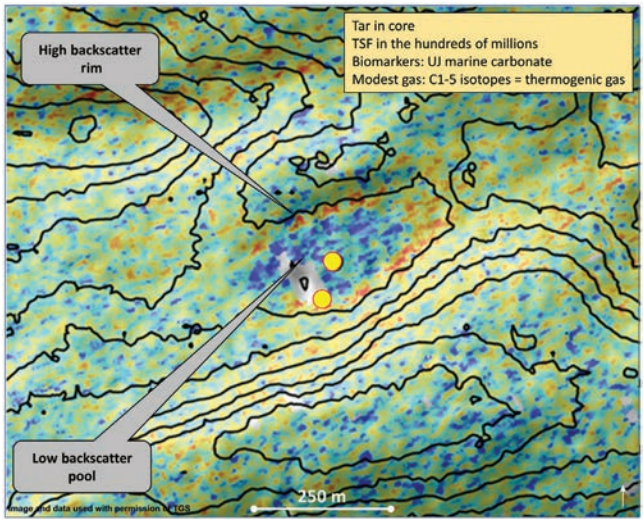

Figure 13. The MBES backscatter map of an oval feature 450 m long and 250 m wide (approximately 70,000 m^2) interpreted to be a brine pool with a high backscatter rim and low backscatter center pool. Two cores, yellow dots, were acquired from this feature, one from the center and one from the rim. Contour interval is 10 m.

has not been seen or reported anywhere else in the world to our knowledge. The term popcorn was given to this unique feature by the Fugro at sea team of Dr. Kelley Brumley and Mr. Adrian Digby. The term is applied to a texturally mottled sea floor commonly with a downslope flow pattern. Popcorn texture is mostly a bathymetric feature with little or no consistently anomalous backscatter.

Based solely on the MBES data, our initial working hypothesis was that the popcorn textured flow features were cored by submarine gas hydrate glaciers. From our 21 cores into popcorn fields, only 1 core recovered hydrates; however, 12 cores recovered tar. Currently, our leading hypothesis is that the popcorn texture is caused by tar flows at the sea bottom. The tar interpretation is consistent with the general observations that tar has little or no anomalous backscatter signature, cores are mostly without chemosynthetic shell fragments, and core geochemistry contains minimal gas. We offer no further interpretation for the origin of the popcorn surface texture at this time.

Figure 15 shows an example of a popcorn field covering approximately 400 km^2 that we interpret to have flowed downslope to the south-southwest, and then ponding against an east–west ridge. Bathymetrically, the popcorn field stands approximately 10 m above the surrounding sea bottom and individual mounds are generally less than 4 m high. Three cores were taken from this feature. Two cores recovered tar with TSF values up to 1.2 billion, and background to minimal levels of gas. GeoMark Research biomarker data correlated the source of the tar to an Upper Jurassic marine carbonate. The third core, to the southwest taken specifically to evaluate an area of particularly low backscatter, had TSF values only slightly elevated over background (40.0–78,000, n = 3 samples) and background levels of total alkane gases (<42 ppmV).

Figure 16 shows another example of popcorn texture. The popcorn field appears to have a flow texture emanating from a northwest–southeast-trending fault zone near the base of the bathymetric high and flowing downslope to the southeast. The flow is approximately 1.2 km wide and 1.5 km long. The field stands between 25 and 40 m above the surrounding sea bottom. The one core from this feature contained no tar, but yielded TSF values of up to 13.6 million, and minimal levels of thermogenic gas. Biomarkers again indicated an Upper Jurassic marine carbonate source facies.

Fault traces

Faults can act as seals and as conduits for fluid migration. In the latter, fracture permeability provides a pathway for fluids to leak to the surface, and the observation of hydrocarbons leaking to the surface along faults from reservoirs is well documented (Boles et al., 2004). In the marine world, faults intersect the sea floor in linear to curvilinear traces that can generally be mapped with high-resolution MBES data, especially if the fault produces bathymetric relief on the sea bottom. Fault traces provide favorable locations to explore for hydrocarbon seepage, but even along the fault traces, seepage targets tend to be concentrated in relatively small point sources

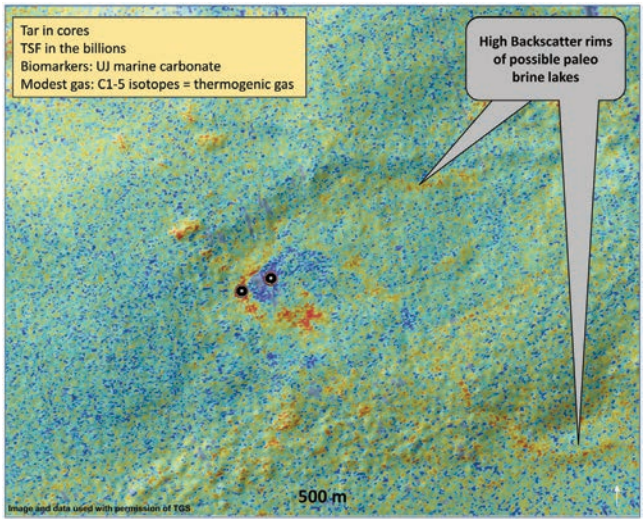

Figure 14. The MBES backscatter map of a crudely circular feature 500 m long and 450 m wide (approximately 270,000 m^2) interpreted to be a brine pool with a high backscatter rim and low backscatter center pool. Two cores were again acquired from this feature, one from the center and one from the rim.

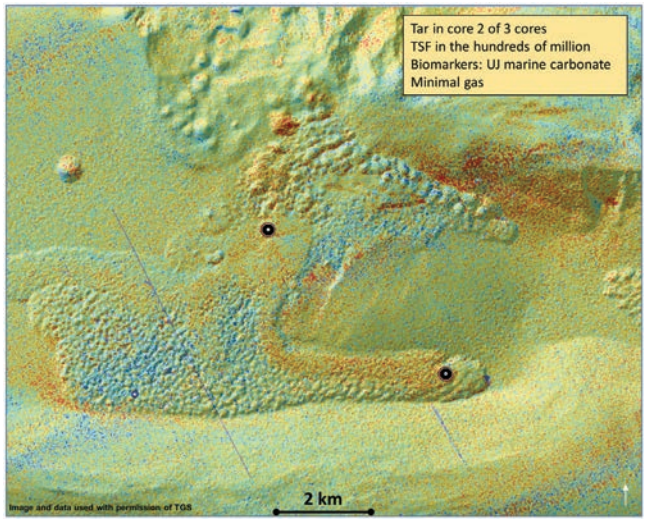

Figure 15. The MBES backscatter map of one of the larger popcorn fields. Three piston cores were acquired in this feature. The northern core was acquired at the projected intersection of a prominent gas plume with the sea bottom. There was no anomalously high backscatter at this location and the core recovered no anomalous amounts of gas. The core contained very soft gray to gray brown clay with pebble size pieces of tar and semi-solid oil and smelled of H_2S gas. The southeastern core near the terminus of the interpreted flow was in a relatively smooth region of the field with moderately high backscatter. The core contained brown clay with pebble size pieces of low-density tar. The third core was taken to the southwest in an area of very low backscatter and mottled surface texture. This core consisted of soft gray clay with a faint H_2S odor.

separated, commonly in our experience, by long distances with no apparent backscatter or water column anomalies along the fault. Key indicators of hydrocarbon seepage along a fault trace are the same as other seep targets discussed herein, specifically, semicircular or flow-shaped regions of high backscatter, mounds, pock marks, or mud volcanoes, although typically modified by or conforming to local bathymetric highs and lows created by the faulting.

Figure 17 shows a zone of intersecting fault traces on the seafloor. Individual faults show a left-stepping geometry, where the fault movement and step overs create local parallelogram-shaped lows. This indicates that the step overs are releasing bends, and therefore, these faults make up left lateral strike slip fault system. Three cores were acquired in this field of view, all located along traces of the fault where water column anomalies indicated gas plume clusters. The northwest core had TSF values of up to 45 million, and total alkane gases of up to 1000 ppmV. GeoMark Research typed the oil biomarkers to an Upper Jurassic marine carbonate. The southwest core had TSF values of up to 45 million, total alkane gases up to 28,000 ppmV, and C_1–C_5 isotopes indicating a thermogenic origin. Oil biomarkers indicated a Tertiary paralic/deltaic source facies. The eastern core had TSF values up to 50 million with minimal gas and heavily biodegraded thermogenic oil. It is unusual, from our experience in basins around the world, to have closely spaced seeps on the same fault system yield biomarker results indicative of different source facies, but in areas of the GOM, multiple petroleum systems can overlap and produce seepage independent from one another (Kennicutt et al., 1992).

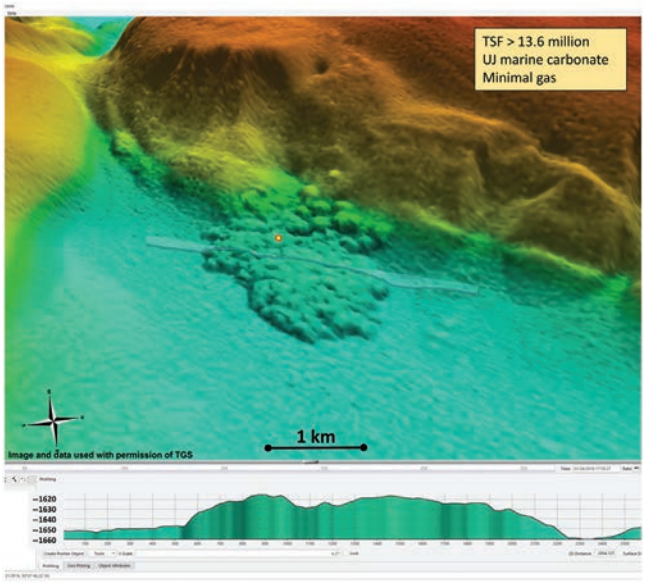

Figure 16. The 3D view of popcorn feature on the sea bottom; 3× vertical exaggeration. Core location is shown with the yellow dot. Core consisted of soft green gray clay with moderate H_2S odor.

Figure 18 shows the locations of three cores acquired on the crest of an anticline along a left lateral strike slip fault system (again interpreted based upon step over/releasing geometries). The north and south cores were acquired along the surface trace of the fault on local backscatter anomalies and where water column

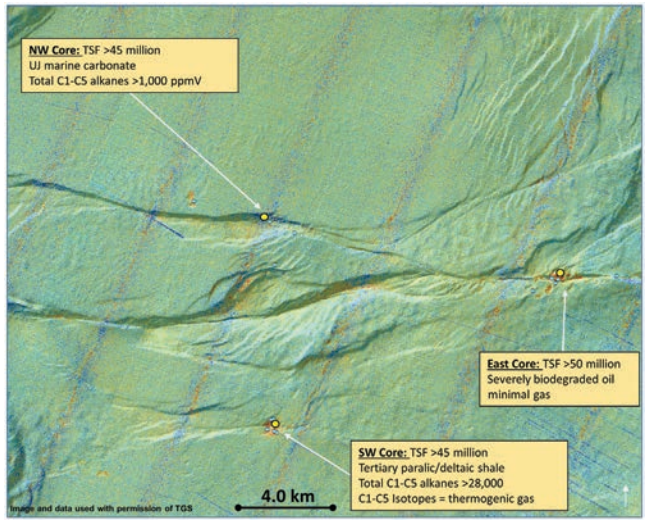

Figure 17. The MBES backscatter map of east–west-trending fault zone. Cores (yellow dots) taken at locations of gas plume touchdown locations (blue dots). All three cores consisted of soft gray clay with H_2S odor. One core had gas expansion features and two of the cores were oil stained.

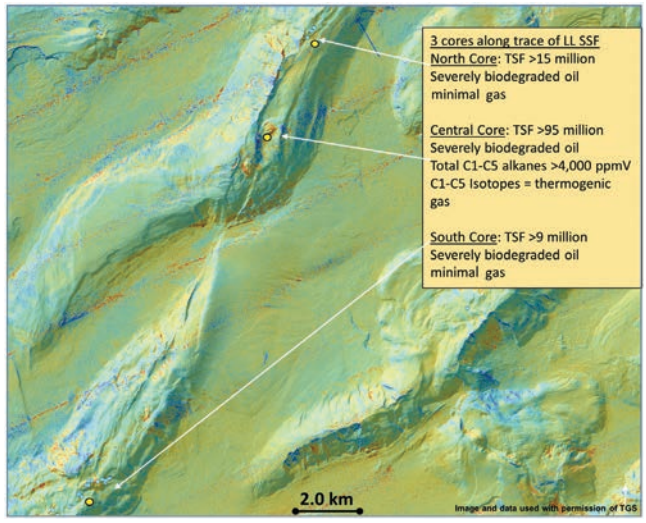

Figure 18. The MBES backscatter map showing a section of a regional left-lateral strike-slip fault zone. Three cores were taken along the fault trace, two at concentrations of gas plumes. The southern core was from a high backscatter area and consisted of green gray mud with sand, shells, and rock fragments. The central core was taken at a moderately high backscatter mound within the fault zone near the crest of an anticline. The core consisted of green gray oil-stained clay. The northern core consisted of green gray clay with faint H_2S odor.

anomalies indicated gas seep clusters; the southern core also is associated with a high-angle fault that cuts across the anticline. All three cores had TSF values in the millions but were all severely biodegraded and resulted in no meaningful biomarker source rock fingerprints. Gas was at background levels in the north and south cores, which is curious as these core targets were picked in the middle of gas plume clusters. We attribute failing to recover cores with high gas values from areas identified by WCAs as due to the inherent inaccuracy of projecting the gas plume to the sea bottom and the areally limited effect of gas seepage on sediment surrounding the location of the seep. The central core had total alkane gases of more than 4000 ppmV, and C_1–C_5 gas isotopes indicated a thermogenic origin for those gases.

Anticlinal crests

Anticlinal crests are bathymetric features of folded strata, commonly with a curvilinear ridgeline on the sea bottom. In our surveys, we have documented many cases in which local patches of anomalously high backscatter occur on the crest of anticlines, with large areas of the fold's surface devoid of anomalous backscatter or water column anomalies. As with faults, we interpret seepage on anticlines to be from point sources which produce semicircular or flow-like regions of high backscatter. Anticlines seen on the sea bottom can be exposed structures from an earlier period of deformation, but in areas of exploration focus by the oil industry, anticlines are more commonly evolving modern or active strain features. As such, their topographic growth can cause gravitational instability resulting in slumping along the crest or steep flanks of the anticline. Slump scarps are excellent targets for hydrocarbon seepage due to their lower lithostatic pressure created by the rapid removal of sediment due to slumping and because the base of slump head scarps provides a topographic inflection point that allows over pressured fluids to focus for seepage (because the ocean is at constant head everywhere and the concave upward headscarp base is a constant head surface; Orange and Breen, 1992; Orange et al., 1994).

Figure 19 shows a north–south anticlinal structure approximately 5 km wide and 30 km long, with a large east-directed slump beginning near to the crest of the anticline. The east facing slope of the anticline is approximately 13°; if slope failure was solely due to the presence of shallow overpressure, a λ of 0.75–0.85 would be sufficient to trigger failure (λ is the dimensionless pore pressure ratio, varying from 0.56, assuming a bulk density of 0.84 g/cm^3 and 50% porosity. These λ values assume an angle of internal friction of 30°–40°; Orange and Breen, 1992.). Two cores were acquired from the anticline, the northern core from the head of the slump and the likely origin of the high backscatter flow, and the southern core from a relatively small pock mark, approximately 150 m in diameter and having slightly elevated backscatter in the center. The northern core taken near the highest part of the high backscatter flow pattern had TSF values of up to 2.2 million and C_1–C_5 of up to 47,000 ppmV. Biomarkers indicated that the source of the oil was Tertiary paralic/deltaic shale. The southern core had TSF values of up to 800,000 and only background levels of gas.

Figure 20 shows the seafloor expression of an anticline approximately 3 km wide and 45 km long. Cores were taken at two locations near the crest of the anticline, each with clusters of gas plumes emanating from patches of high backscatter. Note that seafloor anoma-

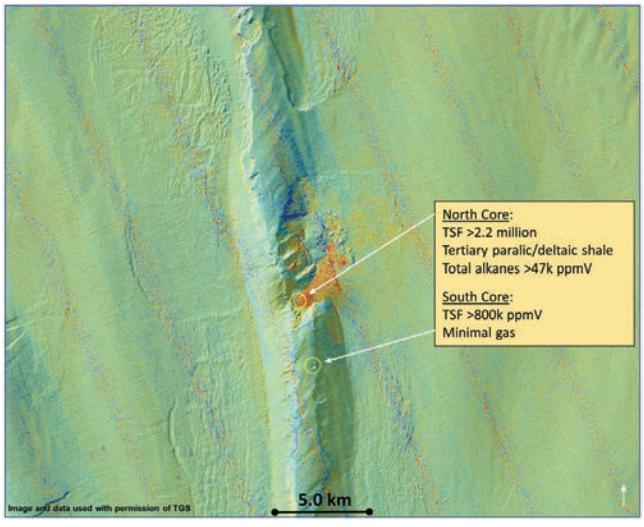

Figure 19. The MBES backscatter map of an anticlinal structure with two cores. The southern core was taken in a small pock mark with high backscatter at the base of the depression. The core consisted of green gray clay and sandy mud with faint H_2S odor. The northern core was taken along the headscarp of a high backscatter slump. The core consisted of green gray clay with H2S odor and gas fractures.

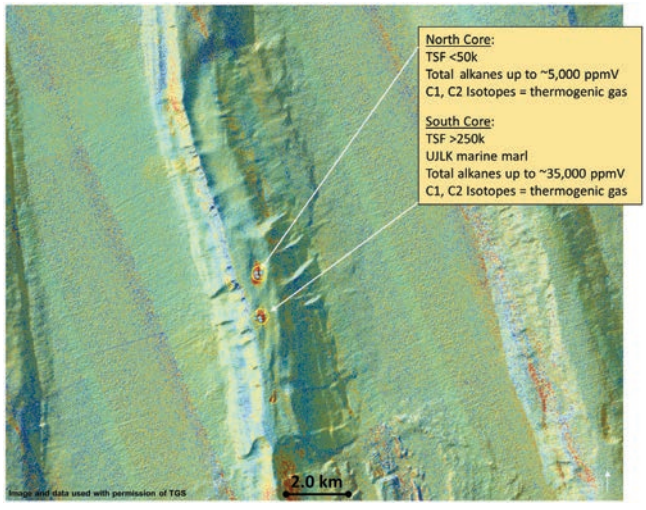

Figure 20. The MBES backscatter image of an anticlinal structure with two cores acquired at very high backscatter areas with gas plume clusters at the crest of the anticline. Both cores consisted of green gray sandy mud with shell fragments and H_2S odor.

lies and associated water column anomalies occur along anticlinal crest-parallel depressions that suggest either a keystone graben or possible lateral strain; either implies areas of local extensional strain that would facilitate seepage. The core to the north had surprisingly low TSF for such a high-quality seep target. Total alkane gases were up to just more than 5000 ppmV and isotopes indicated a thermogenic origin. The core to the south had moderately high TSF of up to approximately 250,000, high total alkane gases, and undegraded biomarkers suggestive of an Upper Jurassic to Lower Cretaceous marine marl source for the oil.

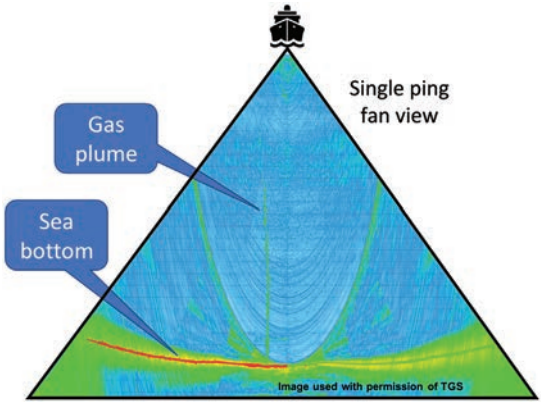

Figure 21. Image is of a single ping water column screen capture showing composite of a single sonar ping and several hundred returns from the sea bottom and water column. A prominent gas plume is shown as a well-defined near vertical green feature emanating from the sea bottom.

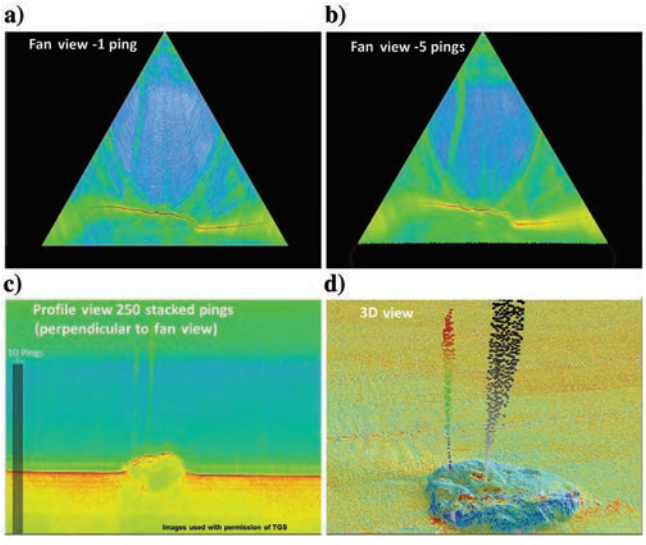

Figure 22. Four images of gas seepage from one feature on the sea bottom. (a) A single ping with a somewhat indistinct plume on the left side of the triangle (the fan pattern of a single ping across track). (b) A combination of five pings, which reinforces the visibility of the plume. (c) A stacked profile view, looking at approximately 250 pings perpendicular to the fan view (perpendicular to the ship track) showing two plumes emanating from a mounded bathymetric feature on the sea bottom. (d) A 3D view showing the plumes and the potential source vent areas of high backscatter.

Water column anomalies

Water column anomalies caused by gas plumes are common features in the GOM (Garcia-Pineda et al., 2016). Gas plumes are unlike all other disturbances observed in the water column, and they are easily seen in the multibeam data as narrow elongate upward features (Figure 21). They are generally not perfectly vertical features but tend to shift laterally as they rise through the water column as they are affected by moving currents. As such, gas plumes can be seen at different depths from one sonar ping to the next.

The projected sea bottom location of water column anomalies created by gas plumes from hydrocarbon seeps becomes a priority target for core sampling and geochemistry. Figure 22 includes four images, reflections of a single sonar ping (Figure 22a), five sonar pings added together to improve clarity of anomalies (Figure 22b), multiple stacked ping profiles shown perpendicular to fan views (Figure 22c), and a 3D perspective showing backscatter on the sea bottom and likely touchdown points of the gas plume (Figure 22d). The process of defining a core target on the sea bottom uses all four types of images. First, the water column is surveyed ping by ping and/or in groups of pings in fan view. When water column anomalies are identified, they are reviewed in profile view to confirm quality and orientation of the anomaly. Finally, the anomaly is viewed in three dimensions with sea bottom data to project the WCA to the sea bottom and to pinpoint the core target location on the sea bottom.

In the TGS MBES mapping program in the GOM 3276, water column anomalies were interpreted to be gas plumes emanating from the sea bottom. Of those, 191 were repeat observations of the same plume on multiple MBES passes (Figure 23). Approximately 50 times where we made a second MBES pass over a previously mapped a plume, there was no plume present on the repeat pass. This observation supports the concept that the gas seepage is not only ephemeral in a geologic time frame (Roberts and Carney, 1997) but also episodic on a daily/weekly time frame.

Figure 24 shows a cluster of water column anomalies interpreted to represent gas plumes (blue dots) and a core (red dot) taken in a high backscatter patch of sea bottom associated with the southwest termination of a north-northeast/south-southwest lineation; the blue dots represent our interpreted touch down points for each WCA. The total alkane gas values from three core samples range from 50,000 to 95,000 ppmV of >98% thermogenic methane. The core was oil stained with TSF values of up to 114 million and biomarkers indicative of a Cretaceous marine shale.

Overall, the TGS program collected 268 cores and analyzed 835 samples from gas plume locations in

the GOM. Most of the cores contained oil and gas indicators; 15 cores were oil stained, 63 cores contained tar, and 22 cores contained gas hydrates (approximately 30% higher than the GOM in general). Geochemically for the gas analyses, the average total alkane gases were just under 40,000 ppmV with 95% of the samples having $C_1 > 90\%$ and 43% having $C_1 > 99\%$. For the oil extract analysis, the TSF averaged more than 54 million for all samples (more than 12 million for only the samples without tar), with 40% of the samples having TSF > 1 million and 67% having TSF > 100,000.

Discussion

It is important to recognize that TGS GOM Seep Survey systematically mapped and evaluated the entire deepwater GOM deeper than 750 m water depth at a very high resolution with a consistent technology, sampling strategy, and analytical program. The seep features, gas plumes, and geochemistry shown here are selected examples from the entire GOM. They represent our best effort to characterize the great majority of seep target types proven by their core geochemistry to be associated with hydrocarbon expulsion at the sea bottom. It is equally important to recognize that the primary tool that we used for selecting targets for coring is sonar. Sonar data allow us to recognize plume features in the water column and acoustically anomalous regions of sea bottom, but it is not a direct hydrocarbon indicator and if seepage leaves no acoustic evidence, we will likely miss those seeps. It is unlikely that we missed many water column anomalies because they are objective features in the water column data and less prone to interpretation. But it is common for hydrocarbon seepage to occur at the sea bottom with no associated gas plume and therefore no WCA to identify. Seep targets interpreted from bathymetry and backscatter data are more subjective and biased by the knowledge and beliefs of the interpreter. As such, the targets that we selected for coring were heavily weighted toward anomalous regions of high sonar backscatter. Even on features with compelling bathymetric expression, such as mud volcanoes, anticlinal crests, fault scarps, and pock marks, we almost exclusively pick coring targets in regions of those features with the highest backscatter. High backscatter, especially when used with bathymetry and geologic intuition, has a proven track record for differentiating locations of oil and gas seepage from areas of little or no seepage. However, as we have seen in the GOM survey, heavy oil, tar, asphalt, etc. without associate gas, typically have a low to mottled backscatter signature and without some other characteristics like popcorn texture, can be difficult to identify as coring targets with multibeam sonar.

Acknowledgments

We would like to acknowledge TGS for allowing us to publish some results from their seep surveys in the GOM. K. Abdallah, C. Corona, D. Bate, and T. Neugebauer were our key contacts at TGS and true believers in seep surveys as valuable exploration tools. A. Ali monitored survey operations and deliverables for TGS.

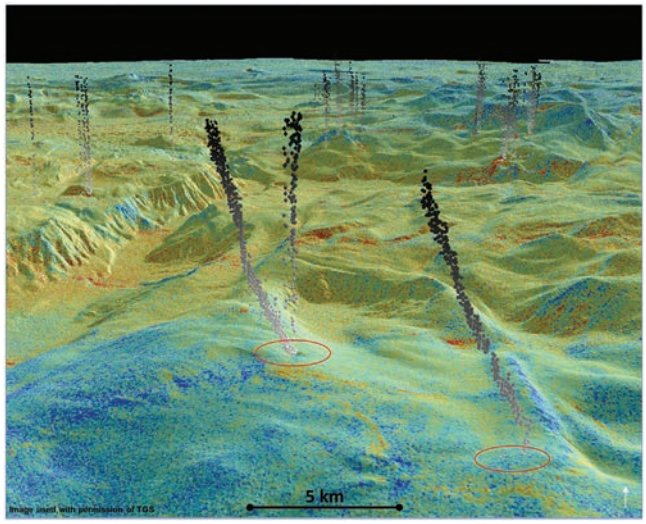

Figure 23. The 3D MBES backscatter image of gas plumes observed on multiple MBES vessel passes. Map shows mostly near vertical gas plumes with two plumes in the foreground (red ovals show approximate touchdown locations on the sea bottom) being inclined significantly from vertical that were observed on a second MBES pass over the area. The plume on the right was only observed on the second pass and not on the first pass. The plume on the left was observed on both passes. One core acquired at the location of the left with the double plumes. The core consisted mostly of gray clay with gas expansion features and an H_2S odor. TSF values were all high, up to almost 400,000 units and total alkane gases of up to 57,000 ppmV (98% thermogenic methane).

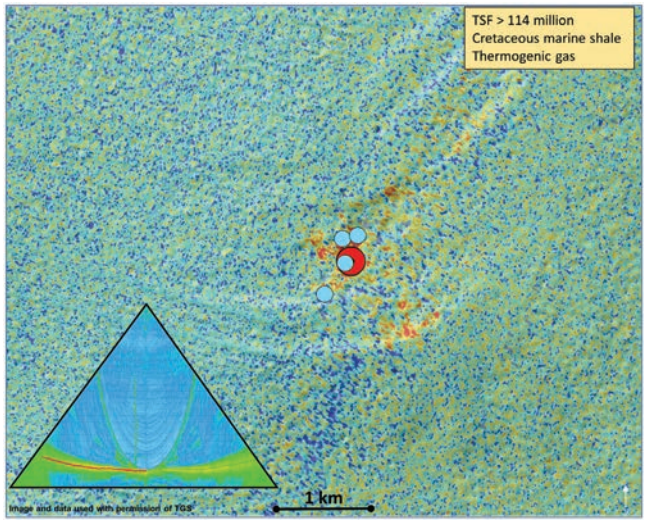

Figure 24. The MBES backscatter map of a moderately elevated backscatter anomaly. Four gas plumes have been interpreted to have their sea bottom origin in the high backscatter region. One core from this location consisted of green gray clay with rock fragments, H_2S odor, and oil staining.

MBES data were acquired by Fugro. Operations managers at Fugro included J. (Jim) Gharib, D. Keener, and D. Almeida. The Fugro at sea MBES processing and interpretation team and party chiefs, in particular, C. Trebaol, K. Brumley, A. Digby, G. Mitchel, and D. Pryne, worked with our team on a daily basis to ensure the highest quality products. Cores were acquired and analyzed by the team at TDI-Brooks International, including J. Brooks, D. Brooks, B. Bernard, M. Kullman, P. Hitchcock, B. Dolan, L. Bender, J. Dickinson, and N. Clark. J. Zumberge and the staff of GeoMark Research provided the biomarker data and interpretations.

Data and materials availability

Data associated with this research are confidential and cannot be released.

References

Bernard, B. B., J. M. Brooks, and W. M. Sackett, 1976, Natural gas seepage in the Gulf of Mexico: Earth and Planet Science Letters, **31**, 48–54, doi: 10.1016/0012-821X(76)90095-9.

Boles, J. R., P. Eichhubl, G. Garven, and J. Chen, 2004, Evolution of a hydrocarbon migration pathway along basin-bounding faults: Evidence from fault cement: AAPG Bulletin, **88**, 947–970, doi: 10.1306/02090403040.

Brooks, J. M., T. J. Bright, B. B. Bernard, and C. R. Schwab, 1979, Chemical aspects of a brine pool at the East Flower Garden bank, northwestern Gulf of Mexico: Limnology and Oceanography, **24**, 735–745, doi: 10.4319/lo.1979.24.4.0735.

Brooks, J. M., M. E. Kennicutt, I. R. MacDonald, D. L. Wilkinson, N. L. Guinasso, and R. R. Bidigare, 1989, Gulf of Mexico hydrocarbon seep communities — Part 4: Descriptions of known chemosynthetic communities: Presented at the Offshore Technology Conference Annual Meeting.

Cole, G. A., A. Yu, F. Peel, C. H. Taylor, R. Requejo, J. DeVay, J. M. Brooks, B. B. Bernard, J. Zumberge, and S. Brown, 2001, The deepwater GOM petroleum system: Insights from piston coring, defining seepage, anomalies, and background: Presented at the 21st Annual GCSSEPM Foundation Research Conference.

Davison, I., J. Pindell, and J. Hull, 2021, The basins, orogens and evolution of the southern Gulf of Mexico and Northern Caribbean: Geological Society of London, Special Publications 504, 1–27.

De Beukelaer, S. M., I. R. MacDonald, N. L. Guinasso, and J. A. Murray, 2003, Distinct side-scan sonar, RADARSAT SAR, and acoustic profiler signatures of gas and oil seeps on the Gulf of Mexico slope: Geo-Marine Letters, **23**, 177–186, doi: 10.1007/s00367-003-0139-9.

Garcia-Pineda, O., I. R. Macdonald, M. Silva, W. Shedd, S. Daneshgar Asl, and B. Schumaker, 2016, Transience and persistence of natural hydrocarbon seepage in Mississippi Canyon, Gulf of Mexico: Deep-Sea Research II, **129**, 119–129, doi: 10.1016/j.dsr2.2015.05.011.

Garcia-Pineda, O., I. R. MacDonald, B. Zimmer, W. Shedd, and H. Roberts, 2010, Remote-sensing evaluation of geophysical anomaly sites in the outer continental slope, northern Gulf of Mexico: Deep Sea Research II, **57**, 1859–1869, doi: 10.1016/j.dsr2.2010.05.005.

Joye, S. B., I. R. MacDonald, J. P. Montoya, and M. Peccini, 2005, Geophysical and geochemical signatures of Gulf of Mexico seafloor brines: Biogeosciences, **2**, 295–309, doi: 10.5194/bg-2-295-2005.

Kennicutt, M. C., T. J. MacDonald, P. A. Comet, G. J. Denoux, and J. M. Brooks, 1992, The origins of petroleum in the northern Gulf of Mexico: Geochimica et Cosmochimica Acta, **56**, 1259–1280, doi: 10.1016/0016-7037(92)90061-M.

MacDonald, I. R., O. Garcia-Pineda, A. Beet, S. Daneshgar Asl, L. Feng, G. Graettinger, D. French-McCay, J. Holmes, C. Hu, F. Huffer, I. Leifer, F. Muller-Karger, A. Solow, M. Silva, and G. Swayze, 2015, Natural and unnatural oil slicks in the Gulf of Mexico: Journal of Geophysical Research: Oceans, **120**, 1–17, doi: 10.1002/2015JC011062.

MacDonald, I. R., J. F. Reilly, N. L. Guinasso, J. M. Brooks, R. S. Carney, W. A. Bryant, and T. J. Bright, 1990, Chemosynthetic mussels at a brine-filled pockmark in the northern Gulf of Mexico: Science, **248**, 1096–1099, doi: 10.1126/science.248.4959.1096.

Newton, R. S., R. C. Cunningham, and C. E. Schubert, 1980, Mud volcanoes and pockmarks: Seafloor engineering hazards or geologic curiosities?: Proceedings of the Annual Offshore Technology Conference, 425–435.

Orange, D. L., R. S. Anderson, and N. A. Breen, 1994, Regular canyon spacing in the submarine environment: The link between hydrology and geomorphology: GSA Today, **4**, 29–39.

Orange, D. L., and N. A. Breen, 1992, The effects of fluid escape on accretionary wedges — 2: Seepage force, slope failure, headless submarine canyons and vents: Journal of Geophysical Research, **97**, 9277–9295, doi: 10.1029/92JB00460.

Roberts, H. H., and R. S. Carney, 1997, Evidence of episodic fluid, gas, and sediment venting on the northern Gulf of Mexico continental slope: Economic Geology Bulletin, **92**, 863–879, doi: 10.2113/gsecongeo.92.7-8.863.

Scanlon, K. M., F. C. Coleman, and C. C. Koenig, 2005, Pockmarks on the outer shelf in the Northern Gulf of Mexico: Gas-release features or habitat modifications by fish?: American Fisheries Society Symposium 41, 301–312.